5. Li Y, Rinne JO, Mosconi L, Pirraglia E, Rusinek H, DeSanti S, Kemppainen N, Nagren K, Kim BC, Tsui W, de Leon MJ (2008) Regional analysis of FDG and PIB-PET images in normal aging, mild cognitive impairment, and Alzheimer's disease. Eur J Nucl Med Mol Imaging 35:2169–2181
6. McFadzean R, Brosnahan D, Hadley D, Mutlukan E (1994) Representation of the visual field in the occipital striate cortex. Br J Ophthalmol 78:185–190
7. Ng SY, Villemagne VL, Masters CL, Rowe CC (2007) Evaluating atypical dementia syndromes using positron emission tomography with carbon 11 labeled Pittsburgh Compound B. Arch Neurol 64:1140–1144
8. Renner JA, Burns JM, Hou CE, McKeel DW Jr, Storandt M, Morris JC (2004) Progressive posterior cortical dysfunction: a clinicopathologic series. Neurology 63:1175–1180
9. Tang-Wai DF, Graff-Radford NR, Boeve BF, Dickson DW, Parisi JE, Crook R, Caselli RJ, Knopman DS, Petersen RC (2004) Clinical, genetic, and neuropathologic characteristics of posterior cortical atrophy. Neurology 63:1168–1174
10. Tenovuo O, Kemppainen N, Aalto S, Nagren K, Rinne JO (2008) Posterior cortical atrophy: a rare form of dementia with in vivo evidence of amyloid-beta accumulation. J Alzheimers Dis 15:351–355

Original article

Nuclear Medicine Communications

Competition between ^{11}C-raclopride and endogenous dopamine in Parkinson's disease

Kenji Ishibashi[a,b], Kenji Ishii[b], Keiichi Oda[b], Hidehiro Mizusawa[a] and Kiichi Ishiwata[b]

Objective **The aim of this study was to understand whether the increase in ^{11}C-raclopride binding in the striatum of patients with Parkinson's disease (PD) is associated with the depletion of endogenous dopamine.**

Methods **Positron emission tomography (PET) scans of the two dopamine D_2 receptor ligands, ^{11}C-raclopride and ^{11}C-*N*-methylspiperone (^{11}C-NMSP), and the dopamine transporter ligand, ^{11}C-2β-carbomethoxy-3β-(4-fluorophenyl)-tropane, were performed on five patients with PD and seven controls. The binding of each tracer was calculated by using a (region–cerebellum)/cerebellum ratio in the caudate, anterior putamen, and posterior putamen.**

Results **In patients with PD, the ^{11}C-raclopride to ^{11}C-NMSP ratios in the posterior putamen, which was the subregion of the striatum with the lowest binding of ^{11}C-2β-carbomethoxy-3β-(4-fluorophenyl)-tropane, were the largest among all three subregions of the striatum. In controls, the ^{11}C-raclopride to ^{11}C-NMSP ratios in all three subregions of the striatum were within a constant range.**

Conclusion **In patients with PD, the kinetic difference between ^{11}C-raclopride and ^{11}C-NMSP was found prominently in the posterior putamen, in which presynaptic degeneration occurred most profoundly. Therefore, we concluded that the increase in ^{11}C-raclopride binding in the striatum of patients with PD was strongly associated with the depletion of endogenous dopamine. ^{11}C-NMSP can be chosen in the place of ^{11}C-raclopride in cases in which it may be essential to eliminate the influence of endogenous dopamine.** ***Nucl Med Commun*** **00:000–000 © 2010 Wolters Kluwer Health | Lippincott Williams & Wilkins.**

Nuclear Medicine Communications 2010, 00:000–000
31(2): 159-166

Keywords: ^{11}C-2β-carbomethoxy-3β-(4-fluorophenyl)-tropane, ^{11}C-*N*-methylspiperone, ^{11}C-raclopride, endogenous dopamine, Parkinson's disease, positron emission tomography

[a]Department of Neurology and Neurological Science, Graduate School, Tokyo Medical and Dental University and [b]Positron Medical Center, Tokyo Metropolitan Institute of Gerontology, Tokyo, Japan

Correspondence to Kiichi Ishiwata, MD, Positron Medical Center, Tokyo Metropolitan Institute of Gerontology, 1-1 Nakacho, Itabashi-ku, Tokyo 173-0022, Japan
Tel: +81 3 3964 3241; fax: +81 3 3964 2188; e-mail: ishiwata@pet.tmig.or.jp

Received 9 September 2009 **Revised** 5 October 2009
Accepted 6 October 2009

Introduction

Among positron emission tomography (PET) radioligands for mapping postsynaptic dopamine D_2 receptors (D_2Rs) in the striatum, carbon-11-labeled raclopride is most often used as a standard D_2R ligand because of its high selectivity [1,2]. We have reported the coupling of age-related decline in postsynaptic D_2Rs and presynaptic dopamine transporters (DATs) in the striatum of normal individuals by using PET with ^{11}C-raclopride and ^{11}C-2β-carbomethoxy-3β-(4-fluorophenyl)-tropane (^{11}C-CFT), respectively [3]. The binding of the two tracers correlated well, irrespective of age. In contrast, our preliminary findings revealed that compared with the binding of ^{11}C-raclopride, the binding of ^{11}C-*N*-methylspiperone (^{11}C-NMSP), another radioligand for mapping D_2Rs, correlates more strongly with that of ^{11}C-CFT in normal individuals (unpublished data). The difference between the two D_2R ligands, ^{11}C-raclopride and ^{11}C-NMSP, can be explained by the variable binding of ^{11}C-raclopride in response to changes in the concentrations of endogenous dopamine caused by various physiological factors. The above concept is based on the following findings: (i) several studies with ^{3}H-labeled ligands explain the differences in the in-vivo binding properties of the two D_2R ligands [4–9]. Specifically, the binding of ^{11}C-raclopride to the D_2Rs in the striatum is reversible in the time frame of a PET scan and competitive with that of endogenous dopamine. In contrast, the binding of ^{11}C-NMSP is substantially irreversible in the time frame of a PET scan and not competitive with that of endogenous dopamine. Consequently, the binding of ^{11}C-raclopride is affected by the concentration of endogenous dopamine, whereas that of ^{11}C-NMSP is not; (ii) considerable interindividual and intraindividual variabilities in the concentration of endogenous dopamine in individuals with normal nigrostriatal dopaminergic function has been reported in earlier studies on the measurements of dopamine metabolites in cerebrospinal fluid [10–12].

On the basis of the above findings, the binding of ^{11}C-raclopride could be relatively higher than that of ^{11}C-NMSP in the striatum of patients with PD, on account of the depletion of endogenous dopamine and preserved D_2Rs in the striatum [13–15]. Moreover, the differences

0143-3636 © 2010 Wolters Kluwer Health | Lippincott Williams & Wilkins

DOI: 10.1097/MNM.0b013e328333e3cb

in the binding levels of the two D_2R ligands among the different subregions of the striatum could be greater in the following order: the posterior putamen > anterior putamen > caudate, corresponding to the reported order of the extent of presynaptic degeneration [16–20]. However, contrary to these considerations, Kaasinen *et al.* [21] reported that the increased binding of ^{11}C-raclopride in patients with PD did not result from the reduction in the amount of endogenous dopamine, but from the upregulation of the D_2Rs. Their conclusion is questionable in light of the binding properties of radioligands described above [4–9] and earlier reports on morphological studies, which state that parkinsonian symptoms appear when 80% of the striatal dopamine is lost [15].

The aim of this study was to understand whether the increase in ^{11}C-raclopride binding in the striatum of patients with PD is associated with the depletion of endogenous dopamine. For this purpose, we performed both ^{11}C-raclopride and ^{11}C-NMSP PET scans on patients with PD and the differences in the binding of the two radioligands were evaluated, particularly in the subregions of the striatum, in relation to the presynaptic functionality evaluated with the binding of ^{11}C-CFT. To confirm the reliability of this study, we performed region of interest (ROI) analysis by using anatomical standardization and coregistration of the images, as objectively as possible.

Materials and methods

Participants

A total of 27 individuals (five patients with PD and 22 healthy volunteers) participated in this retrospective study. We divided the 22 healthy volunteers into three groups (first group: seven, second group: eight, third group: seven), and the five patients with PD were classified into the third group. In the first group, seven volunteers [four men and three women; age, 55–68 years (mean=60.6, SD=5.4)] underwent static PET scans of ^{11}C-raclopride to create the ^{11}C-raclopride template. In the second group, eight volunteers [8 men; age, 20–22 years (mean=20.6, SD=0.7)] underwent dynamic PET scans of ^{11}C-NMSP to ascertain the method for static PET scans that represent ^{11}C-NMSP binding to the D_2Rs, as we had earlier validated static PET scans for both ^{11}C-raclopride and ^{11}C-CFT [3,22]. In the third group, five patients with PD [two men and three women; age, 53–67 years (mean=57.8, SD=5.5)] and seven volunteers [7 men; age, 21–23 years (mean=22.3, SD=1.0)] underwent three static PET scans of ^{11}C-raclopride, ^{11}C-NMSP, and ^{11}C-CFT. A magnetic resonance imaging (MRI) scan of the brain was performed on all participants to check for the abnormal lesion. All volunteers were defined as healthy on the basis of their medical history, the results of their physical and neurological examination performed by neurologists, and the findings of the MRI that were reported by the radiologists. None of the volunteers was on any medication at the time of this study. All patients were drug naive at the time of the study. Table 1 shows the demographic data of the patients. This study protocol was approved by the Ethics Committee of the Tokyo Metropolitan Institute of Gerontology. Written informed consent was obtained from all participants of this study.

Table 1 Clinical features of patients with Parkinson's disease

Patient	Sex	Age (years)	Duration (years)	Side[a]	Hoehn–Yahr stage	Symptoms
1	F	54	2	Right	1	Tremor, rigidity
2	F	57	1	Right	1	Tremor
3	M	67	5	Right	2	Tremor, rigidity
4	M	58	1	Right	1	Tremor
5	F	53	2	Left	1	Tremor

F, female; M, male.
[a]Affected side.

Positron emission tomography imaging

PET imaging was performed at the Positron Medical Center, Tokyo Metropolitan Institute of Gerontology by using a SET-2400W scanner (Shimadzu, Kyoto, Japan) in the three-dimensional scanning mode for static scans or the two-dimensional scanning mode for dynamic scans. The transmission data were acquired by using a rotating ^{68}Ga/^{68}Ge rod as a source for attenuation correction. Images with 50 slices were obtained with a resolution of $2 \times 2 \times 3.125$ mm voxels and a 128×128 matrix. ^{11}C-raclopride, ^{11}C-NMSP, and ^{11}C-CFT were prepared by the reaction of ^{11}C-methyl triflate and the respective desmethyl compound as described in earlier studies [23,24].

Dynamic scanning of ^{11}C-NMSP was performed for 90 min after an intravenous bolus injection of 640 ± 67 MBq (mean ± SD). The specific activity ranged from 29.2 to 109.3 GBq/μmol. Static scannings of the three tracers were performed for 40–55, 54–66, and 75–90 min after intravenous bolus injection of ^{11}C-raclopride, ^{11}C-NMSP, and ^{11}C-CFT, respectively. Two PET studies with ^{11}C-raclopride and ^{11}C-CFT were carried out at an interval of 2.5–3 h on the same day, and the study with ^{11}C-NMSP was carried out on another day. The injection doses (mean ± SD) for ^{11}C-raclopride, ^{11}C-NMSP, and ^{11}C-CFT were 298 ± 60, 321 ± 14, and 331 ± 22 MBq, respectively, and the specific activities were 14.0–95.9, 14.5–82.4, and 14.5–68.0 GBq/μmol, respectively, at the time of injection.

Magnetic resonance imaging

The MRI scans were performed at the Tokyo Metropolitan Geriatric Hospital. Transaxial T1-weighted images (three-dimensional spoiled-gradient-recalled echo images; repetition time = 9.2 ms, echo time = 2.0 ms, matrix size = $256 \times 256 \times 124$, voxel size = $0.94 \times 0.94 \times 1.3$ mm) and transaxial T2-weighted images (first spin echo; repetition time = 3000 ms, echo time = 100 ms, matrix size = $256 \times 256 \times 20$, voxel size = $0.7 \times 0.7 \times 6.5$ mm) were obtained by using a 1.5-Tesla Signa EXCITE HD scanner (GE, Milwaukee, Wisconsin, USA).

Analysis of positron emission tomography images

Image manipulations were performed using Dr View version R2.0 (AJS, Tokyo, Japan) and statistical parametric mapping 2 (SPM2; Functional Imaging Laboratory, London, UK) implemented in MATLAB version 7.0.1 (The MathWorks, Natick, Massachusetts, USA). We used SPM2 for the anatomical standardization and coregistration of the obtained images. To eliminate arbitrariness and subjectivity, both of which are disadvantages of conventional ROI analysis in which ROIs are placed individually, and to improve objectivity, we placed ROIs on the same anatomical position for all participants at a time by standardization of each image, as described below.

Creation of the ^{11}C-raclopride template and average MRI image

The ^{11}C-raclopride template, which was used as the standard for brain images in this study, was created from the integral ^{11}C-raclopride images taken from the seven healthy individuals of the first group, as described earlier [25,26]. For this purpose, MRI-based spatial normalization was used. First, individual ^{11}C-raclopride images were coregistered with their corresponding T1-weighted MRI images. Next, individual MRI images were spatially transformed to the SPM2-T1-MRI template. The same deformation parameters were applied to the individual coregistered ^{11}C-raclopride images. Finally, the ^{11}C-raclopride template was made by averaging the transformed ^{11}C-raclopride images of seven healthy individuals and applying a smoothing Gaussian filter (full width at half maximum=8 × 8 × 8 mm). In addition, we obtained the average MRI image by averaging the transformed MRI images of seven healthy individuals.

Creation of normalized images of ^{11}C-raclopride, ^{11}C-NMSP, and ^{11}C-CFT

Individual ^{11}C-raclopride, ^{11}C-NMSP, and ^{11}C-CFT PET images were coregistered. Next, the individual ^{11}C-raclopride images were anatomically normalized to the standard brain images by using the ^{11}C-raclopride template described above which was developed in-house. The same deformation parameters were applied to the individual coregistered ^{11}C-NMSP and ^{11}C-CFT images. Subsequently, we obtained the individual normalized PET images of ^{11}C-raclopride, ^{11}C-NMSP, and ^{11}C-CFT. All the normalized PET images and the average MRI image were anatomically the same.

Uptake ratio index of ^{11}C-raclopride, ^{11}C-NMSP, and ^{11}C-CFT

We placed the ROIs on the average MRI image: one ROI with an 8-mm diameter was placed on the caudate, one ROI with an 8-mm diameter on the anterior putamen, and one ROI with an 8-mm diameter on the posterior putamen on both sides in each of five contiguous slices. A total of 30 ROIs with 10-mm diameter were placed throughout the cerebellar cortex in three contiguous slices. These ROIs placed on the average MRI were spatially moved on each normalized PET image.

To evaluate the binding of ^{11}C-raclopride, ^{11}C-NMSP, and ^{11}C-CFT to their respective binding sites, we calculated the uptake ratio index (URI) by the following formula [18,27]: URI=[(activity in each region) − (activity in the cerebellum)]/[(activity in the cerebellum)]. Earlier, we had validated the use of the URI as a method to estimate the binding potential of ^{11}C-raclopride and ^{11}C-CFT [3,22].

The following two analysis methods were performed. First, we compared the three tracers in both patients with PD and healthy volunteers, using the URI of every ROI placed on the striatum. Second is the comparison of the ipsilateral and contralateral sides to the predominant symptoms in patients with PD.

Relationship between binding of ^{11}C-NMSP to D_2Rs and uptake ratio index

To validate the use of the URI for ^{11}C-NMSP, we examined the correlation between the binding of ^{11}C-NMSP to the D_2Rs (association constant, k_3) and the URI in eight healthy volunteers of the second group. Six ROIs were placed on the striatum of each dynamic scanned participant. The k_3 was estimated by graphical analysis of irreversible ligands, using the cerebellum as a reference [28,29]. The cerebellum was selected as a reference region in the analysis because the density of D_2Rs and serotonin 5-HT_2 receptors in this region is negligible. The URI of each ROI was also estimated, as described above. Next, we compared the k_3 values of total 48 ROIs with the URI.

Statistics

The differences in averages and variances were tested by Student's t-test and one-way analysis of variance, respectively. Correlations between the two groups were assessed by linear regression analysis with Pearson's correlation test. P values less than 0.01 were considered statistically significant.

Results

There was a significant positive linear correlation between k_3 and the URI of ^{11}C-NMSP (r=0.98; $P < 0.0001$), as shown in Fig. 1. Therefore, the URI was adopted for further analyses.

In normal individuals (Fig. 2), the URI of ^{11}C-raclopride correlated significantly with that of ^{11}C-CFT in the posterior putamen, but not in the other two subregions. Conversely, the URI of ^{11}C-NMSP correlated significantly with that of ^{11}C-CFT in all three subregions.

In patients with PD (Fig. 3), a negative correlation (r=0.71; $P < 0.0001$) was found between the URI of

^{11}C-raclopride and that of ^{11}C-CFT in the three subregions of the striatum. The URI of ^{11}C-CFT was smaller in the following order: the posterior putamen < anterior putamen < caudate, whereas the URI of ^{11}C-raclopride was larger as follows: the posterior putamen > anterior putamen > caudate. In contrast, a very small positive correlation (r=0.29; P=0.0003) between the URI of ^{11}C-NMSP and that of ^{11}C-CFT in the three subregions was found. Thus, the URI of ^{11}C-NMSP was almost constant, irrespective of that of ^{11}C-CFT in the three subregions. Each average ligand image (Fig. 4), which was made by averaging the URI images of five patients with PD, revealed the apparent tendencies of the three ligands.

To evaluate the more detailed regional differences in the ^{11}C-raclopride and ^{11}C-NMSP binding in the three subregions of the striatum, ratios of the URI of ^{11}C-raclopride to that of ^{11}C-NMSP (R/N ratios) were plotted, as shown in Fig. 5. In normal individuals, the R/N ratios in all three subregions of the striatum were maintained in a constant range. Conversely, in patients with PD, the R/N ratios were significantly higher in the following order: the posterior putamen > anterior putamen > caudate.

Table 2 shows the comparison in the URI of three tracers between the contralateral and ipsilateral sides to the predominant symptoms in patients with PD. For ^{11}C-raclopride, the contralateral URI in all subregions of the striatum tended to be larger than the ipsilateral URI. For both ^{11}C-NMSP and ^{11}C-CFT, the contralateral URI in all subregions of the striatum tended to be smaller than the ipsilateral URI.

Fig. 1

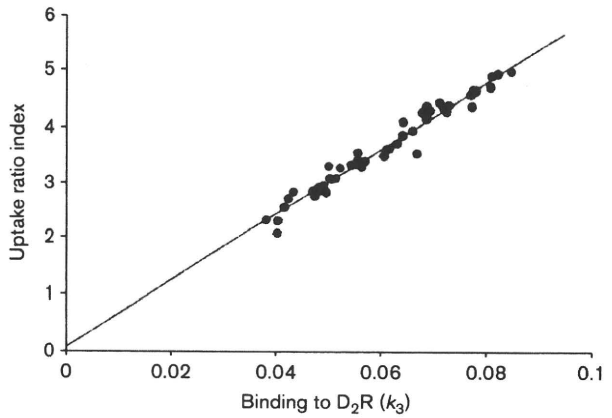

Correlation between the binding to D_2 receptors (D_2R) [association constant (k_3)] and uptake ratio index of ^{11}C-*N*-methylspiperone in the striatum. The solid line represents the regression line. Linear correlation is significant (r=0.98; P<0.0001).

Discussion

In this study, we investigated whether the increase of ^{11}C-raclopride binding in the striatum of patients with PD is associated with the depletion of endogenous dopamine by examining the PET scans of ^{11}C-raclopride, ^{11}C-NMSP, and ^{11}C-CFT in normal individuals and patients with PD.

In normal individuals, earlier neuroimaging studies reported that there was a significant linear correlation between DATs and D_2Rs in the three subregions of the striatum, irrespective of age [3,30]. This study showed

Fig. 2

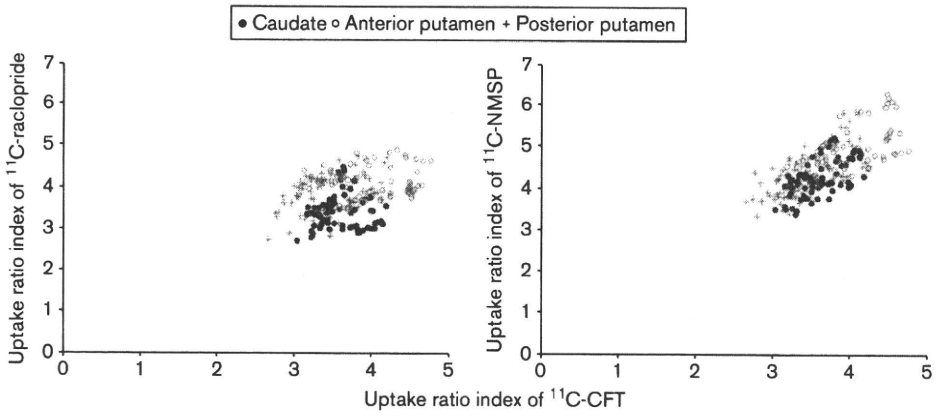

Correlation between the uptake ratio indices of ^{11}C-2β-carbomethoxy-3β-(4-fluorophenyl)-tropane (^{11}C-CFT) and ^{11}C-raclopride (left) and between the uptake ratio indices of ^{11}C-CFT and ^{11}C-*N*-methylspiperone (^{11}C-NMSP) (right) in controls. Closed circles, open circles, and plus signs represent the caudate, anterior putamen, and posterior putamen, respectively. In the graph on the left, a significant correlation is shown only in the posterior putamen (r=0.37, P=0.002). In the graph on the right, there are significant correlations in the caudate (r=0.60, P<0.0001), anterior putamen (r=0.67, P<0.0001), and posterior putamen (r=0.69, P<0.0001).

Fig. 3

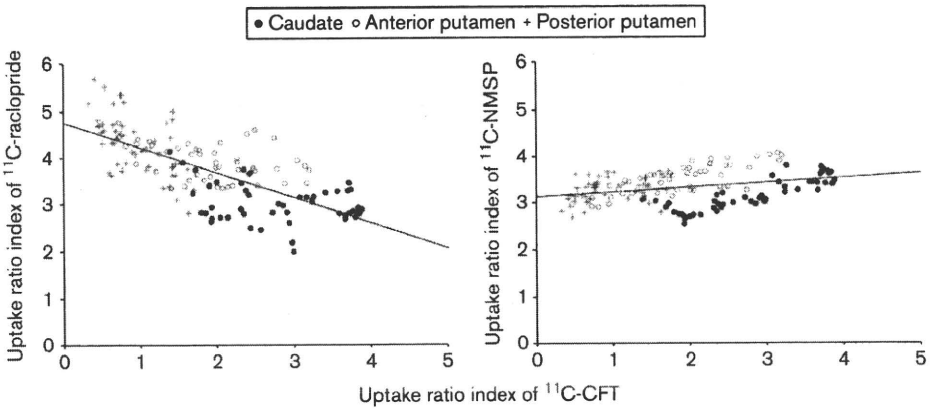

Correlations between the uptake ratio indices of ^{11}C-2β-carbomethoxy-3β-(4-fluorophenyl)-tropane (^{11}C-CFT) and ^{11}C-raclopride (left) and between the uptake ratio indices of ^{11}C-CFT and ^{11}C-*N*-methylspiperone (^{11}C-NMSP) (right) in patients with Parkinson's disease. Closed circles, open circles, and plus signs represent the caudate, anterior putamen, and posterior putamen, respectively. The solid lines represent the regression line for all plots combined with all subregions. Linear correlation is significant in the graph on the left (r=0.71; P<0.0001) and in the graph on the right (r=0.29; P=0.0003).

Fig. 4

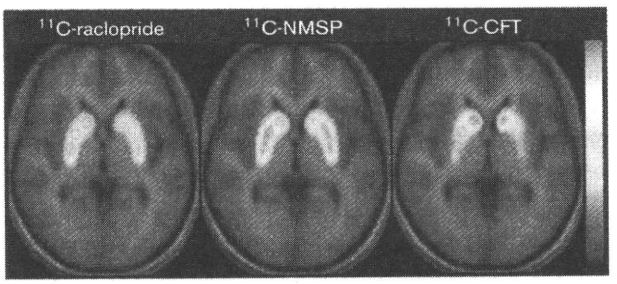

The average ligand images of each tracer superimposed on the average magnetic resonance imaging image at the level of the basal ganglia in patients with Parkinson's disease (PD). Each average ligand image was made by averaging the uptake ratio index images of five patients with PD and clipping the striatum. The binding of ^{11}C-raclopride has an inverse relationship with that of ^{11}C-2β-carbomethoxy-3β-(4-fluorophenyl)-tropane (^{11}C-CFT). The binding of ^{11}C-*N*-methylspiperone (^{11}C-NMSP) was fairly uniform in all subregions of the striatum. For demonstration, the right side of the regions of interest placed on the striatum (the caudate, anterior putamen, and posterior putamen) is displayed.

Fig. 5

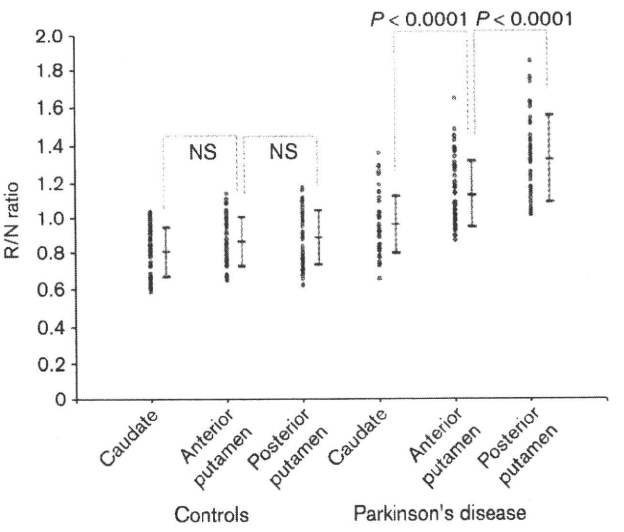

Uptake ratio indices of ^{11}C-raclopride to that of ^{11}C-*N*-methylspiperone (R/N ratios) in the caudate, anterior putamen, and posterior putamen. In controls, the R/N ratios are maintained within a constant range. In patients with Parkinson's disease, the R/N ratios are significantly greater in the following order: the posterior putamen, anterior putamen, and caudate. NS, not significant.

that the URI of ^{11}C-CFT in the three subregions of the striatum was more strongly associated with that of ^{11}C-NMSP than that of ^{11}C-raclopride (Fig. 2). As described in the Introduction, the different binding properties between the two D_2R ligands were considered to be a result of the variability in the binding of ^{11}C-raclopride, in response to changes in the endogenous dopamine concentrations caused by various physiological factors.

Figures 3 and 4 showed that in patients with PD the URI of ^{11}C-raclopride in the three subregions had an inverse relationship with that of ^{11}C-CFT. Morphological and neuroimaging studies for PD have established the following: (i) neuronal loss begins in the lateral ventral nigra, which projects toward the posterior putamen, and throughout the illness this region remains the most severely affected [31,32]. (ii) Severe dopamine depletion was found in the posterior putamen with relative sparing of the caudate nucleus [15]. (iii) DAT levels correlate

Table 2 The uptake ratio index of three ligands in patients with Parkinson's disease

	Caudate			Anterior putamen			Posterior putamen		
	Ipsilateral	Contralateral		Ipsilateral	Contralateral		Ipsilateral	Contralateral	
	Mean ± SD	Mean ± SD	*P* value	Mean ± SD	Mean ± SD	*P* value	Mean ± SD	Mean ± SD	*P* value
^{11}C-raclopride	2.95 ± 0.45	3.05 ± 0.41	0.40	3.92 ± 0.38	3.93 ± 0.33	0.91	4.18 ± 0.62	4.39 ± 0.35	0.38
^{11}C-NMSP	3.19 ± 0.36	3.09 ± 0.31	0.02	3.59 ± 0.24	3.40 ± 0.32	0.08	3.30 ± 0.12	3.21 ± 0.13	0.35
^{11}C-CFT	2.97 ± 0.72	2.63 ± 0.87	0.03	2.21 ± 0.57	1.57 ± 0.48	0.03	1.20 ± 0.37	0.70 ± 0.02	0.02

^{11}C-CFT, ^{11}C-2β-carbomethoxy-3β-(4-fluorophenyl)-tropane; ^{11}C-NMSP, ^{11}C-*N*-methylspiperone. *P* values were obtained by the paired Student's *t*-test performed on ipsilateral and contralateral sides.

with the striatal dopamine concentrations [33]. On the basis of these studies, the results derived from Figs 3 and 4 suggested that the more the dopamine concentrations in the striatum decrease, the higher the binding of ^{11}C-raclopride is. Conversely, the URI of ^{11}C-NMSP in all subregions of the striatum was almost constant, irrespective of the URI of ^{11}C-CFT. In fact, a small but significant correlation was found between the two, and the slope of the regression line was very small.

To evaluate the different properties of the two D_2R ligands more clearly, we used the R/N ratio, which is an independent parameter irrespective of age (Fig. 5). In normal individuals, the R/N ratios in the three subregions of the striatum were maintained within a constant range. In contrast, in patients with PD, the R/N ratios exhibited obvious increase in the following order: the posterior putamen, anterior putamen, and caudate. In other words, the more the dopamine concentrations in the striatum decrease, the greater is the difference between the binding of ^{11}C-raclopride and ^{11}C-NMSP.

These results in this study showed that the kinetic difference between ^{11}C-raclopride and ^{11}C-NMSP was found predominantly in the posterior putamen, in which dopamine depletion and presynaptic degeneration were found to be most severe [15–20]. In addition, earlier in-vitro and in-vivo studies have revealed that endogenous dopamine concentrations affect the binding of ^{11}C-raclopride, but not of ^{11}C-NMSP in the striatum [4–9, 34–36]. Therefore, on the basis of our results and earlier studies, we suggested that in patients with PD, the depletion of endogenous dopamine is strongly associated with the increase in ^{11}C-raclopride binding, especially in the posterior putamen. In addition, we suggested that ^{11}C-NMSP can be chosen in place of ^{11}C-raclopride in cases in which it may be essential to eliminate the influence of endogenous dopamine.

Earlier, a study on the direct comparison of ^{11}C-raclopride and ^{11}C-NMSP in seven patients with early PD was reported by Kaasinen *et al.* [21]. They compared the binding of the two D_2R ligands on the contralateral side to the symptoms with that on the ipsilateral side, and found that the binding of both ^{11}C-raclopride and ^{11}C-NMSP on the contralateral side was 105% of that on the opposite side. They concluded that the binding of the two D_2R ligands increased because of the upregulation of the D2Rs, and suggested that the increased binding of ^{11}C-raclopride did not result from reduced concentrations of endogenous dopamine. In this study (Table 2), for the binding of ^{11}C-raclopride we found a similar tendency as observed in the case of Kaasinen *et al.* and other earlier reports on the binding of ^{11}C-raclopride in patients with early PD [37–39]. However, contrary to the result of Kaasinen *et al.* for the binding of ^{11}C-NMSP, our data showed that the contralateral side tended to be smaller than the ipsilateral side in all subregions of the striatum, although there were no significant differences between the values of both sides. Regarding the binding of ^{11}C-NMSP in patients with PD, because there have been only a few studies with a small number of patients, consistent side-to-side differences about its binding have not been known [29,40]. For the binding of ^{11}C-CFT, the contralateral side in each subregion was smaller than the opposite and the difference in the posterior putamen was the largest as reported in earlier reports [19,20].

We are unable to clearly explain the essential difference between the findings reported by Kaasinen *et al.* [21] and these findings. However, we have obtained sound results on the basis of the earlier in-vivo and in-vitro properties of ^{11}C-raclopride and ^{11}C-NMSP, as described earlier [4–9, 34–36]. In addition, the binding properties of the two D_2R ligands were normalized by the binding of ^{11}C-CFT. It is also noteworthy that this study was performed not only with better spatial resolution of the PET scanner to enable subregional analyses of the striatum, but also with more advanced ROI analysis based on the PET–MRI coregistration technique so that the objectivity was as high as possible, compared with that in early studies [21,29,40]. The drawbacks of this study may be a small number of patients with PD and no age-matched control for patients with PD, although our data are enough to achieve our purpose.

Conclusion

We evaluated ^{11}C-raclopride, ^{11}C-NMSP, and ^{11}C-CFT PET scans in normal individuals and patients with PD. In controls, the URI of ^{11}C-CFT in all subregions of the striatum was more strongly associated with that of ^{11}C-NMSP than that of ^{11}C-raclopride. In patients with PD,

the URI of ^{11}C-raclopride in the posterior putamen, in which the presynaptic degeneration occurred most profoundly in the striatum, was relatively higher than that of ^{11}C-NMSP. These findings showed that different concentrations of endogenous dopamine had different effects on the binding properties of the two D_2R ligands. Therefore, we concluded that the increase in ^{11}C-raclopride binding in the striatum of patients with PD is strongly associated with the depletion of endogenous dopamine. ^{11}C-NMSP can be chosen in place of ^{11}C-raclopride in cases in which it may be essential to eliminate the influence of endogenous dopamine.

Acknowledgements

The authors are grateful to Mr Keiichi Kawasaki and Ms Hiroko Tsukinari for their technical assistance and insightful discussions. This study was supported by a Grant-in-Aid for Scientific Research (B) No. 20390334 by the Japan Society for the Promotion of Science (JSPS).

References

1 Farde L, Pauli S, Hall H, Eriksson L, Halldin C, Hogberg T, *et al.* Stereoselective binding of 11C-raclopride in living human brain – a search for extrastriatal central D2-dopamine receptors by PET. *Psychopharmacology (Berl)* 1988; **94**:471–478.

2 Kohler C, Hall H, Ogren SO, Gawell L. Specific in vitro and in vivo binding of 3H-raclopride. A potent substituted benzamide drug with high affinity for dopamine D-2 receptors in the rat brain. *Biochem Pharmacol* 1985; **34**:2251–2259.

3 Ishibashi K, Ishii K, Oda K, Kawasaki K, Mizusawa H, Ishiwata K. Regional analysis of age-related decline in dopamine transporters and dopamine D2-like receptors in human striatum. *Synapse* 2009; **63**:282–290.

4 Hall H, Wedel I, Halldin C, Kopp J, Farde L. Comparison of the in vitro receptor binding properties of N-[3H]methylspiperone and [3H]raclopride to rat and human brain membranes. *J Neurochem* 1990; **55**:2048–2057.

5 Inoue O, Kobayashi K, Tsukada H, Itoh T, Langstrom B. Difference in in vivo receptor binding between [3H]N-methylspiperone and [3H]raclopride in reserpine-treated mouse brain. *J Neural Transm Gen Sect* 1991; **85**:1–10.

6 Young LT, Wong DF, Goldman S, Minkin E, Chen C, Matsumura K, *et al.* Effects of endogenous dopamine on kinetics of [3H]N-methylspiperone and [3H]raclopride binding in the rat brain. *Synapse* 1991; **9**:188–194.

7 Terai M, Hidaka K, Nakamura Y. Comparison of [3H]YM-09151-2 with [3H]spiperone and [3H]raclopride for dopamine d-2 receptor binding to rat striatum. *Eur J Pharmacol* 1989; **173**:177–182.

8 Seeman P, Guan HC, Niznik HB. Endogenous dopamine lowers the dopamine D2 receptor density as measured by [3H]raclopride: implications for positron emission tomography of the human brain. *Synapse* 1989; **3**:96–97.

9 Hall H, Farde L, Sedvall G. Human dopamine receptor subtypes – in vitro binding analysis using 3H-SCH 23390 and 3H-raclopride. *J Neural Transm* 1988; **73**:7–21.

10 Ishibashi K, Kanemaru K, Saito Y, Murayama S, Oda K, Ishiwata K, *et al.* Cerebrospinal fluid metabolite and nigrostriatal dopaminergic function in Parkinson's disease. *Acta Neurol Scand.* (in press).

11 Seeldrayers P, Messina D, Desmedt D, Dalesio O, Hildebrand J. CSF levels of neurotransmitters in Alzheimer-type dementia. Effects of ergoloid mesylate. *Acta Neurol Scand* 1985; **71**:411–414.

12 Hildebrand J, Bourgeois F, Buyse M, Przedborski S, Goldman S. Reproducibility of monoamine metabolite measurements in human cerebrospinal fluid. *Acta Neurol Scand* 1990; **81**:427–430.

13 Guttman M, Seeman P, Reynolds GP, Riederer P, Jellinger K, Tourtellotte WW. Dopamine D2 receptor density remains constant in treated Parkinson's disease. *Ann Neurol* 1986; **19**:487–492.

14 Bokobza B, Ruberg M, Scatton B, Javoy-Agid F, Agid Y. [3H]spiperone binding, dopamine and HVA concentrations in Parkinson's disease and supranuclear palsy. *Eur J Pharmacol* 1984; **99**:167–175.

15 Kish SJ, Shannak K, Hornykiewicz O. Uneven pattern of dopamine loss in the striatum of patients with idiopathic Parkinson's disease. Pathophysiologic and clinical implications. *N Engl J Med* 1988; **318**:876–880.

16 Morrish PK, Sawle GV, Brooks DJ. An [18F]dopa-PET and clinical study of the rate of progression in Parkinson's disease. *Brain* 1996; **119 (Pt 2)**:585–591.

17 Brooks DJ, Ibanez V, Sawle GV, Quinn N, Lees AJ, Mathias CJ, *et al.* Differing patterns of striatal 18F-dopa uptake in Parkinson's disease, multiple system atrophy, and progressive supranuclear palsy. *Ann Neurol* 1990; **28**:547–555.

18 Frost JJ, Rosier AJ, Reich SG, Smith JS, Ehlers MD, Snyder SH, *et al.* Positron emission tomographic imaging of the dopamine transporter with 11C-WIN 35 428 reveals marked declines in mild Parkinson's disease. *Ann Neurol* 1993; **34**:423–431.

19 Nurmi E, Bergman J, Eskola O, Solin O, Vahlberg T, Sonninen P, *et al.* Progression of dopaminergic hypofunction in striatal subregions in Parkinson's disease using [18F]CFT PET. *Synapse* 2003; **48**:109–115.

20 Rinne JO, Ruottinen H, Bergman J, Haaparanta M, Sonninen P, Solin O. Usefulness of a dopamine transporter PET ligand [(18)F]beta-CFT in assessing disability in Parkinson's disease. *J Neurol Neurosurg Psychiatry* 1999; **67**:737–741.

21 Kaasinen V, Ruottinen HM, Nagren K, Lehikoinen P, Oikonen V, Rinne JO. Upregulation of putaminal dopamine D2 receptors in early Parkinson's disease: a comparative PET study with [11C] raclopride and [11C]N-methylspiperone. *J Nucl Med* 2000; **41**:65–70.

22 Hashimoto M, Kawasaki K, Suzuki M, Mitani K, Murayama S, Mishina M, *et al.* Presynaptic and postsynaptic nigrostriatal dopaminergic functions in multiple system atrophy. *Neuroreport* 2008; **19**:145–150.

23 Langer ONK, Dolle F, Lundkvist C, Sandell J, Swahn CG, Vaufrey F, *et al.* Precursor synthesis and radiolabelling of the dopamine D2 receptor ligand [11C]raclopride from [11C]methyl triflate. *J Labelled Comp Radiopharm* 1999; **42**:1183–1193.

24 Kawamura K, Oda K, Ishiwata K. Age-related changes of the [11C]CFT binding to the striatal dopamine transporters in the Fischer 344 rats: a PET study. *Ann Nucl Med* 2003; **17**:249–253.

25 Meyer JH, Gunn RN, Myers R, Grasby PM. Assessment of spatial normalization of PET ligand images using ligand-specific templates. *Neuroimage* 1999; **9**:545–553.

26 Gispert JD, Pascau J, Reig S, Martinez-Lazaro R, Molina V, Garcia-Barreno P, *et al.* Influence of the normalization template on the outcome of statistical parametric mapping of PET scans. *Neuroimage* 2003; **19**:601–612.

27 Antonini A, Leenders KL, Reist H, Thomann R, Beer HF, Locher J. Effect of age on D2 dopamine receptors in normal human brain measured by positron emission tomography and 11C-raclopride. *Arch Neurol* 1993; **50**:474–480.

28 Wong DF, Wagner HN Jr, Dannals RF, Links JM, Frost JJ, Ravert HT, *et al.* Effects of age on dopamine and serotonin receptors measured by positron tomography in the living human brain. *Science* 1984; **226**: 1393–1396.

29 Hagglund J, Aquilonius SM, Eckernas SA, Hartvig P, Lundquist H, Gullberg P, *et al.* Dopamine receptor properties in Parkinson's disease and Huntington's chorea evaluated by positron emission tomography using 11C-N-methyl-spiperone. *Acta Neurol Scand* 1987; **75**:87–94.

30 Volkow ND, Wang GJ, Fowler JS, Ding YS, Gur RC, Gatley J, *et al.* Parallel loss of presynaptic and postsynaptic dopamine markers in normal aging. *Ann Neurol* 1998; **44**:143–147.

31 Gibb WR, Lees AJ. Anatomy, pigmentation, ventral and dorsal subpopulations of the substantia nigra, and differential cell death in Parkinson's disease. *J Neurol Neurosurg Psychiatry* 1991; **54**:388–396.

32 Fearnley JM, Lees AJ. Ageing and Parkinson's disease: substantia nigra regional selectivity. *Brain* 1991; **114 (Pt 5)**:2283–2301.

33 Bezard E, Dovero S, Prunier C, Ravenscroft P, Chalon S, Guilloteau D, *et al.* Relationship between the appearance of symptoms and the level of nigrostriatal degeneration in a progressive 1-methyl-4-phenyl-1,2,3,6-tetrahydropyridine-lesioned macaque model of Parkinson's disease. *J Neurosci* 2001; **21**:6853–6861.

34 Dewey SL, Smith GS, Logan J, Brodie JD, Fowler JS, Wolf AP. Striatal binding of the PET ligand 11C-raclopride is altered by drugs that modify synaptic dopamine levels. *Synapse* 1993; **13**:350–356.

35 Ishiwata K, Hayakawa N, Ogi N, Oda K, Toyama H, Endo K, *et al.* Comparison of three PET dopamine D2-like receptor ligands, [11C]raclopride, [11C]nemonapride and [11C]N-methylspiperone, in rats. *Ann Nucl Med* 1999; **13**:161–167.

36 Seeman P, Niznik HB, Guan HC. Elevation of dopamine D2 receptors in schizophrenia is underestimated by radioactive raclopride. *Arch Gen Psychiatry* 1990; **47**:1170–1172.

37 Antonini A, Schwarz J, Oertel WH, Beer HF, Madeja UD, Leenders KL. [11C]raclopride and positron emission tomography in previously untreated patients with Parkinson's disease: Influence of L-dopa and lisuride therapy on striatal dopamine D2-receptors. *Neurology* 1994; **44**:1325–1329.

38 Rinne JO, Laihinen A, Rinne UK, Nagren K, Bergman J, Ruotsalainen U. PET study on striatal dopamine D2 receptor changes during the progression of early Parkinson's disease. *Mov Disord* 1993; **8**:134–138.

39 Sawle GV, Playford ED, Brooks DJ, Quinn N, Frackowiak RS. Asymmetrical pre-synaptic and post-synpatic changes in the striatal dopamine projection in dopa naive parkinsonism. Diagnostic implications of the D2 receptor status. *Brain* 1993; **116 (Pt 4)**:853–867.

40 Rutgers AW, Lakke JP, Paans AM, Vaalburg W, Korf J. Tracing of dopamine receptors in hemiparkinsonism with positron emission tomography (PET). *J Neurol Sci* 1987; **80**:237–248.

Acta Neurol Scand 2010: 122: 46–51 DOI: 10.1111/j.1600-0404.2009.01255.x

ACTA NEUROLOGICA
SCANDINAVICA

Cerebrospinal fluid metabolite and nigrostriatal dopaminergic function in Parkinson's disease

Ishibashi K, Kanemaru K, Saito Y, Murayama S, Oda K, Ishiwata K, Mizusawa H, Ishii K. Cerebrospinal fluid metabolite and nigrostriatal dopaminergic function in Parkinson's disease.
Acta Neurol Scand: 2010: 122: 46–51.

Objectives – To evaluate the association between cerebrospinal fluid (CSF) homovanillic acid (HVA) concentrations and nigrostriatal dopaminergic function assessed by positron emission tomography (PET) imaging with carbon-11-labeled 2β-carbomethoxy-3β-(4-fluorophenyl)-tropane (^{11}C-CFT), which can measure the dopamine transporter (DAT) density, in Parkinson's disease (PD). *Methods* – ^{11}C-CFT PET scans and CSF examinations were performed on 21 patients with PD, and six patients with non-parkinsonian syndromes (NPS) as a control group. *Results* – In the PD group, CSF HVA concentrations were significantly correlated with the striatal uptake of ^{11}C-CFT ($r = 0.76$, $P < 0.01$). However, in the NPS group, two indices were within the normal range. *Conclusions* – In PD, CSF HVA concentrations correlate with nigrostriatal dopaminergic function. Therefore, CSF HVA concentrations may be an additional surrogate marker for estimating the remaining nigrostriatal dopaminergic function in case that DAT imaging is unavailable.

K. Ishibashi[1,2], K. Kanemaru[3], Y. Saito[4], S. Murayama[5], K. Oda[2], K. Ishiwata[2], H. Mizusawa[1], K. Ishii[2]

[1]Department of Neurology and Neurological Science, Graduate School, Tokyo Medical and Dental University, Tokyo, Japan; [2]Positron Medical Center, Tokyo Metropolitan Institute of Gerontology, Tokyo, Japan; [3]Department of Neurology, Tokyo Metropolitan Geriatric Hospital, Tokyo, Japan; [4]Department of Pathology, Tokyo Metropolitan Geriatric Hospital, Tokyo, Japan; [5]Department of Neuropathology, Tokyo Metropolitan Institute of Gerontology, Tokyo, Japan

Key words: cerebrospinal fluid; dopamine transporter; homovanillic acid; Parkinson's disease; positron emission tomography; ^{11}C-CFT

Kenji Ishii, MD, Positron Medical Center, Tokyo Metropolitan Institute of Gerontology, 1-1 Nakacho, Itabashi-ku, Tokyo 173-0022, Japan
Tel.: +81 3 3964 3241
Fax: +81 3 3964 2188
e-mail: ishii@pet.tmig.or.jp

Accepted for publication June 25, 2009

Introduction

In humans, homovanillic acid (HVA) is the major end-product of dopamine metabolism. The HVA in the cerebrospinal fluid (CSF) is largely derived from the nigrostriatal dopaminergic pathway; therefore, HVA concentration in the CSF has been used as an index of dopamine synthesis and presumed to reflect nigrostriatal dopaminergic function. However, even with the availability of a rigorous collection protocol, especially with respect to puncture time and pre-procedural resting, considerable inter-individual and intra-individual variability has been reported with regard to the concentration of CSF HVA in subjects with normal nigrostriatal function (1–3). Therefore, the extent to which CSF HVA concentrations reflect the nigrostriatal dopaminergic function is still unknown, and no study has specifically elucidated the association between the concentration of CSF HVA and the function of nigrostriatal dopamine.

Many studies have shown that the concentration of CSF HVA substantially reduces in patients with Parkinson's disease (PD), which is a neurodegenerative disorder caused by nigrostriatal dopaminergic dysfunction (4–12). However, the extent of reduction also varied a great deal among patients with PD. Because of the variability, the relationship of clinical disability with CSF HVA concentrations and the accuracy of CSF HVA concentrations in differentiating PD from other parkinsonian syndromes have yet to be determined. Several authors have reported an inverse relationship between CSF HVA concentrations and the clinical severity (5–7, 10, 11), while others have denied such a relationship (9, 12, 13). Other neurodegenerative disorders caused by the dysfunction of nigrostriatal dopaminergic system, such as multiple system atrophy (MSA), progressive

supranuclear palsy (PSP) and corticobasal degeneration, also show the reductions of CSF HVA concentrations as compared to normal subjects (8, 14, 15). Therefore, the usefulness of measuring CSF HVA concentrations in daily clinical practice has not yet been established.

In order to address the physiological and pathophysiological backgrounds of these issues, we evaluated the correlation between CSF HVA concentrations and nigrostriatal dopaminergic function. Furthermore, we have discussed the mechanism by which the concentration of CSF HVA reduces in patients with PD.

As means of evaluating nigrostriatal dopaminergic function, we performed carbon-11-labeled 2β-carbomethoxy-3β-(4-fluorophenyl)-tropane (^{11}C-CFT) positron emission tomography (PET) scans which can reveal the dopamine transporter (DAT) density in the striatum. DAT imaging has been recognized as a standard marker for the diagnosis of PD, because it is a very sensitive, reproducible, and reliable marker of nigrostriatal dopaminergic function (16–21).

Materials and methods

Subjects

The present study was a retrospective study. The subjects comprised 35 patients [19 men and 16 women; age 60–83 years (mean age = 71.7 years, SD = 6.0)]. They visited the neurological outpatient clinic at Tokyo Metropolitan Geriatric Hospital from April 2001–November 2004. Of the 35 patients, 29 had parkinsonian symptoms and on the basis of each clinical criteria (22–24), 21 were diagnosed with PD, three with MSA, and five with PSP. The remaining six patients had no parkinsonian symptoms: three were clinically diagnosed with Alzheimer's disease (AD), two with spinocerebellar degeneration (SCD), and one with amyotrophic lateral sclerosis (ALS). Table 1 shows the demographic data. The patients with MSA and PSP were classified in the patients with non-PD (NPD) group, while the patients with AD, SCD and ALS were classified in the patients with non-parkinsonian syndromes (NPS) group. The CSF examinations and the ^{11}C-CFT PET scans were performed within 5 months of each other. None of the patients had any concomitant hereditary disorder that could cause parkinsonian symptoms. All the patients were drug naive.

The normal range of HVA was determined by examining the CSF of 13 normal control subjects [five men and eight women; age, 65–88 years (mean = 77.2 years, SD = 8.2)]. Similarly, the normal range for nigrostriatal dopaminergic function was determined by performing ^{11}C-CFT PET scans of eight normal control subjects [five men and three women; age, 55–74 years (mean age = 62.3 years, SD = 6.9)]. All the control subjects were healthy and did not have any underlying diseases or abnormities, as determined on the basis of their medical history and their physical and neurological examinations. None of them were on any medications at the time of the study. All the subjects also underwent routine MRI examinations.

All the CSF examinations and ^{11}C-CFT PET scans were performed for research. This study protocol was approved by the Ethics Committee of the Tokyo Metropolitan Institute of Gerontology and written informed consents were obtained from all the participants.

CSF analysis

Lumbar puncture was performed in the lateral decubitus position to obtain CSF samples from each subject. The first few milliliter of CFS was discarded. The next 3 ml of CFS was used for routine determinations of cell counts, protein and sugar and an additional 2 ml was stored at −70°C until the assays were preformed. The concentration of CSF HVA was measured by injecting 80 μl CSF

Table 1 Demographics of patients and control subjects

	Subjects					
	n	M:F	Age (years)	Duration (years)	Striatal uptake of ^{11}C-CFT (Uptake ratio index)	CSF HVA (ng/ml)
Parkinson's disease	21	11:10	72.9 ± 5.0	1.8 ± 1.3	0.94 ± 0.20	12.8 ± 9.35
Hoehn-Yahr 1	1	1:0	62	1	1.38	36.8
Hoehn-Yahr 2	8	4:4	71.6 ± 4.6	1.4 ± 0.9	1.03 ± 0.14	15.6 ± 9.4
Hoehn-Yahr 3	12	6:6	74.7 ± 3.9	2.1 ± 1.5	0.85 ± 0.17	8.9 ± 5.4
Non-Parkinson's disease	8	4:4	70.5 ± 7.7	1.6 ± 0.8	1.00 ± 0.19	16.4 ± 7.7
Non-parkinsonian syndromes	6	4:2	68.8 ± 6.3	4.5 ± 2.4	2.48 ± 0.28	31.9 ± 13.0
Control for PET study	8	5:3	62.3 ± 6.9		2.68 ± 0.44	
Control for CSF study	13	5:8	77.2 ± 8.2			36.0 ± 13.8

Data are expressed as mean ± SD; *n* = number, CSF, cerebrospinal fluid; HVA, homovanillic acid.

samples into a high-performance liquid chromatography system equipped with 16 electrochemical sensors (CEAS Model 5500; ESA, Bedford, MA, USA), as described previously (14).

PET imaging

^{11}C-CFT PET data acquisition – PET studies were performed at the Positron Medical Center, Tokyo Metropolitan Institute of Gerontology using a SET 2400W scanner (Shimadzu, Kyoto, Japan) in the three-dimensional scanning mode (25). The ^{11}C-CFT was prepared as described previously (26). Each subject received an intravenous bolus injection of 388 ± 75 (mean ± SD) MBq of ^{11}C-CFT. Each subject was then placed in the supine position with their eyes closed in the PET camera gantry. The head was immobilized with a customized head holder in order to align the orbitomeatal line parallel to the scanning plane. To measure the uptake of ^{11}C-CFT, a static scan was performed for 75–90 min after the injection. The specific activity at the time of injection ranged from 7.1–119.6 GBq/μmol. The transmission data were acquired using a rotating ^{68}Ga/^{68}Ge rod source for attenuation correction. Images of 50 slices were obtained with a resolution of 2 × 2 × 3.125 mm voxels and a 128 × 128 matrix.

Analysis of ^{11}C-CFT PET images – Image manipulations were carried out by using the Dr View software (version R2.0; AJS, Tokyo, Japan). The individual PET images were resliced in the transaxial direction, parallel to the anterior–posterior intercommissural (AC–PC) line. Circular regions of interest (ROIs) were placed with reference to the brain atlas and individual MRI images. Five ROIs (diameter, 8 mm) were placed on the striatum on both the left and right sides in each of the three contiguous slices (the AC–PC plane, and regions 3.1 and 6.2 mm above the AC–PC line). Of the five ROIs, one ROI was placed on the caudate and four on the putamen. A total of 50 ROIs (diameter, 10 mm) were selected throughout the cerebellar cortex in five contiguous slices. To evaluate the striatal uptake of ^{11}C-CFT, we calculated the uptake ratio index by the following formula (17, 18), as previously validated (27, 28).

$$\text{Uptake ratio index} = (\text{activity in the striatum} - \text{activity in the cerebellum}) / (\text{activity in the cerebellum}).$$

Statistical analysis

Differences in the averages were tested using a Student's *t*-test. Correlations between the two groups were assessed by linear regression analysis with Pearson's correlation test. $P < 0.01$ was considered to indicate statistical significance.

Results

The inter-individual variability in the concentrations of CSF HVA in each group was relatively large (Fig. 1A). CSF HVA concentrations in both the PD ($P < 0.01$) and NPD groups ($P < 0.01$) were significantly lower than that in the control group (mean ± 2SD, 36.0 ± 27.6), while no significant difference was observed between the NPS and control groups.

The striatal uptake of ^{11}C-CFT in the PD and NPD groups was below the normal range (mean ± 2SD, 2.68 ± 0.87; Fig. 1B). In the PD group, CSF HVA concentrations were significantly

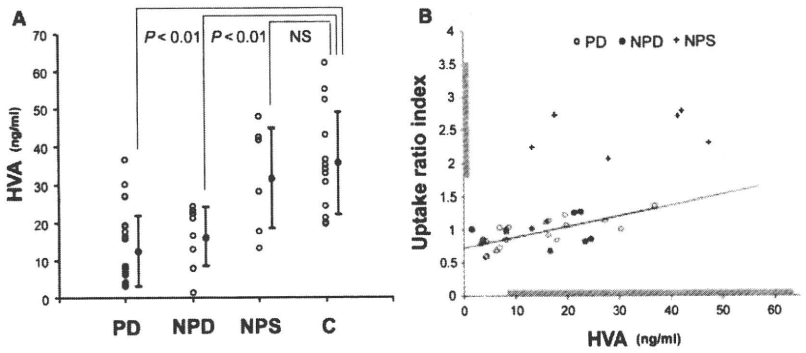

Figure 1. (A) The comparison of CSF HVA concentrations among the disease and control groups. Vertical bars represent mean ± SD. (B) Relationship between CSF HVA concentrations and the striatal uptake of ^{11}C-CFT. A solid line represents the regression line for the PD group. Linear correlation was significant ($r = 0.76$; $P < 0.01$). The grey bars beside the *x*- and *y*-axes represent the normal range (mean ± 2SD) for HVA (36.0 ± 27.6) and the striatal uptake of ^{11}C-CFT (2.68 ± 0.87). PD, Parkinson's disease; NPD, non-Parkinson's disease with parkinsonism; NPS, non-parkinsonian syndromes; C, controls; NS, not significant; CSF, cerebrospinal fluid; HVA, homovanillic acid.

correlated with the striatal uptake of ^{11}C-CFT ($r = 0.76$, $P < 0.01$). In the NPD group, although the correlation between the two indices was not statistically significant, the distribution pattern between the two indexes showed the same tendency as that in the PD group. However, in the NPS group, both CSF HVA concentrations and the striatal uptake of ^{11}C-CFT were within the normal ranges.

Discussion

We evaluated the correlation between CSF HVA concentrations and nigrostriatal dopaminergic function by performing ^{11}C-CFT PET scans. ^{11}C-CFT PET scans showed that all patients with PD and NPD had the dysfunction of nigrostriatal dopaminergic system and all patients with NPS had normal function. The CSF HVA concentrations of all patients with PD and NPD were significantly lower than those of normal subjects, in accordance with previous studies (5–12, 14, 15), whereas, there was no significant difference in CSF HVA concentrations between normal subjects and patients with NPS. These results suggest that CSF HVA concentrations could reflect nigrostriatal dopaminergic function. However, in accordance with previous reports (1–9, 13, 14), all groups showed large inter-individual variability in CSF HVA concentrations and relatively wide overlaps among groups were found. Therefore, in clinical practice, measuring CSF HVA concentrations may be of limited value in the diagnosis of PD.

This is the first study that investigated the correlation between CSF HVA concentrations and nigrostriatal dopaminergic dysfunction. Regardless of relatively high inter-individual variability, CSF HVA concentrations in the PD group showed a considerably high correlation with the striatal uptake of ^{11}C-CFT. The NPD group with nigrostriatal dopaminergic dysfunction showed the same tendency as the PD group, although without significant correlation probably because of the small number of patients. On the other hand, the NPD group with normal nigrostriatal dopaminergic function showed normal ranges in both the HVA level and the striatal uptake of ^{11}C-CFT. Therefore, CSF HVA concentrations may be an additional surrogate maker for estimating the nigrostriatal dopaminergic function in patients with PD, in case that DAT imaging, which has been recognized as a standard maker for the diagnosis of PD, is unavailable.

It is important to note that the DAT images of patients with PD are unique; in the pre-symptomatic phase the reduction in the availability of striatal DAT was detected, presumably as a result of both the degeneration of nigral dopaminergic cells and the compensatory downregulation of DATs on the presynaptic site to maintain normal synaptic dopamine concentrations (17–21). Furthermore, the striatal DAT availability declined at an annual rate of 5–10% (19, 21, 29–31).

Considering our results and the unique characteristics of the DAT images, a possible explanation about the association between CSF HVA concentrations and the striatal uptake of ^{11}C-CFT is as follows (Fig. 2). The first stage of the disease is a compensatory and asymptomatic phase. Along with the progression of nigrostriatal degeneration, the striatal DAT availability begins to decrease, as described earlier (17–21). However, due to several compensatory mechanisms, including the downregulation of DATs and the upregulation of dopamine synthesis, the striatal dopamine concentrations are kept within the normal range (32). As a result, CSF HVA concentrations are also kept in the normal range because CSF HVA is the major end-product of striatal dopamine metabolism. This phase would show relatively large intra-individual and inter-individual variability in CSF HVA concentrations, as observed in subjects with normal nigrostriatal dopaminergic function, because of the reserve capacity for adjusting its levels. The second stage of the progression of the disease is an advanced and symptomatic phase. The compensatory mechanisms to maintain normal synaptic

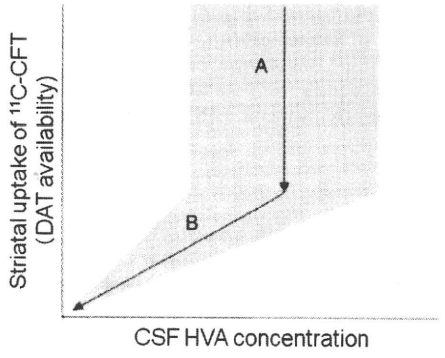

Figure 2. Schematic representation of the mechanism of CSF HVA reduction in patients with PD. (A) The nigrostriatal degeneration begins with a decrease in DAT availability, but due to several compensatory mechanisms, striatal dopamine concentrations (CSF HVA concentrations) are maintained within the normal range. There is a large variability with regard to CSF HVA concentrations. (B) The compensatory mechanisms break down and striatal dopamine concentrations (CSF HVA concentrations) begin to decrease along with the decrease in DAT availability. The variability in CSF HVA concentrations gradually becomes smaller. The grey zone represents the range of variability in CSF HVA concentrations to the striatal uptake of ^{11}C-CFT. DAT, dopamine transporter; CSF, cerebrospinal fluid, HVA, homovanillic acid.

dopamine concentrations break down and the striatal dopamine and CSF HVA concentrations begin to decrease with the reduction of DAT availability. In this phase, the intra-individual and inter-individual variability in CSF HVA concentrations would gradually decrease because of a lesser capacity for adjusting its levels. Consequently, CSF HVA concentrations remain within a narrow range that corresponds to the remaining nigrostriatal dopaminergic function. In symptomatic patients with PD, CSF HVA concentrations correlate with nigrostriatal dopaminergic function. To verify this explanation, a study with larger number of patients is needed.

In conclusion, we found a significant correlation between CSF HVA concentrations and the striatal uptake of ^{11}C-CFT in patients with PD. Although we should remember that CSF HVA concentrations show large variability, CSF HVA concentrations may be an additional surrogate maker for estimating the remaining nigrostriatal dopaminergic function in patients with PD in case that DAT imaging is unavailable.

Acknowledgements

The authors thank Mr Keiichi Kawasaki and Ms Hiroko Tsukinari for their technical assistance. This study was supported by Grants-in-Aid for Neurological and Psychiatric Research (S. Murayama, Y. Saito and K. Ishii) and Research for Longevity (S. Murayama, Y. Saito and K. Ishii) from the Ministry of Health, Labor and Welfare of Japan; for Scientific Research (B) No. 20390334 (K. Ishiwata) from the Japan Society for the Promotion of Science; for the Program for Promotion of Fundamental Studies in Health Sciences of the National Institute of Biomedical Innovation, Japan (No: 06–46, K. Ishiwata); and for Long-Term Comprehensive Research on Age-associated Dementia from the Tokyo Metropolitan Institute of Gerontology (K. Kanemaru, S. Murayama and K. Ishii).

References

1. Seeldrayers P, Messina D, Desmedt D, Dalesio O, Hildebrand J. CSF levels of neurotransmitters in Alzheimer-type dementia. Effects of ergoloid mesylate. Acta Neurol Scand 1985;**71**:411–4.
2. Ballenger JC, Post RM, Goodwin FK. Neurochemistry of cerebrospinal fluid in normal individuals. In: Wood JH, ed. Neurobiology of cerebrospinal fluid. New York: Plenum Press, 1982;**2**:143–55.
3. Hildebrand J, Bourgeois F, Buyse M, Przedborski S, Goldman S. Reproducibility of monoamine metabolite measurements in human cerebrospinal fluid. Acta Neurol Scand 1990;**81**:427–30.
4. Parkinson Study Group. Cerebrospinal fluid homovanillic acid in the DATATOP study on Parkinson's disease. Parkinson Study Group. Arch Neurol 1995;**52**:237–45.
5. Chia LG, Cheng FC, Kuo JS. Monoamines and their metabolites in plasma and lumbar cerebrospinal fluid of Chinese patients with Parkinson's disease. J Neurol Sci 1993;**116**:125–34.
6. Chase TN, Ng LK. Central monoamine metabolism in Parkinson's disease. Arch Neurol 1972;**27**:486–91.
7. Korf J, van Praag HM, Schut D, Nienhuis RJ, Lakke JP. Parkinson's disease and amine metabolites in cerebrospinal fluid: implications for L-Dopa therapy. Eur Neurol 1974; **12**:340–50.
8. Abdo WF, De Jong D, Hendriks JC et al. Cerebrospinal fluid analysis differentiates multiple system atrophy from Parkinson's disease. Mov Disord 2003;**19**:571–9.
9. Davidson DL, Yates CM, Mawdsley C, Pullar IA, Wilson H. CSF studies on the relationship between dopamine and 5-hydroxytryptamine in Parkinsonism and other movement disorders. J Neurol Neurosurg Psychiatry 1977;**40**: 1136–41.
10. Tohgi H, Abe T, Takahashi S, Ueno M, Nozaki Y. Cerebrospinal fluid dopamine, norepinephrine, and epinephrine concentrations in Parkinson's disease correlated with clinical symptoms. Adv Neurol 1990;**53**:277–82.
11. Mayeux R, Stern Y. Intellectual dysfunction and dementia in Parkinson disease. Adv Neurol 1983;**38**:211–27.
12. Gibson CJ, Logue M, Growdon JH. CSF monoamine metabolite levels in Alzheimer's and Parkinson's disease. Arch Neurol 1985;**42**:489–92.
13. Kurlan R, Goldblatt D, Zaczek R et al. Cerebrospinal fluid homovanillic acid and parkinsonism in Huntington's disease. Ann Neurol 1988;**24**:282–4.
14. Kanemaru K, Mitani K, Yamanouchi H. Cerebrospinal fluid homovanillic acid levels are not reduced in early corticobasal degeneration. Neurosci Lett 1998;**245**:121–2.
15. Ruberg M, Javoy-Agid F, Hirsch E et al. Dopaminergic and cholinergic lesions in progressive supranuclear palsy. Ann Neurol 1985;**18**:523–9.
16. Nurmi E, Bergman J, Eskola O et al. Reproducibility and effect of levodopa on dopamine transporter function measurements: a [18F]CFT PET study. J Cereb Blood Flow Metab 2000;**20**:1604–9.
17. Frost JJ, Rosier AJ, Reich SG et al. Positron emission tomographic imaging of the dopamine transporter with 11C-WIN 35,428 reveals marked declines in mild Parkinson's disease. Ann Neurol 1993;**34**:423–31.
18. Wong DF, Yung B, Dannals RF et al. In vivo imaging of baboon and human dopamine transporters by positron emission tomography using [11C]WIN 35,428. Synapse 1993;**15**:130–42.
19. Nurmi E, Bergman J, Eskola O et al. Progression of dopaminergic hypofunction in striatal subregions in Parkinson's disease using [18F]CFT PET. Synapse 2003; **48**:109–15.
20. Rinne JO, Ruottinen H, Bergman J, Haaparanta M, Sonninen P, Solin O. Usefulness of a dopamine transporter PET ligand [(18)F]beta-CFT in assessing disability in Parkinson's disease. J Neurol Neurosurg Psychiatry 1999;**67**:737–41.
21. Nurmi E, Ruottinen HM, Kaasinen V et al. Progression in Parkinson's disease: a positron emission tomography study with a dopamine transporter ligand [18F]CFT. Ann Neurol 2000;**47**:804–8.
22. Hughes AJ, Daniel SE, Kilford L, Lees AJ. Accuracy of clinical diagnosis of idiopathic Parkinson's disease: a clinico-pathological study of 100 cases. J Neurol Neurosurg Psychiatry 1992;**55**:181–4.
23. Litvan I, Agid Y, Calne D et al. Clinical research criteria for the diagnosis of progressive supranuclear palsy (Steele-Richardson-Olszewski syndrome): report of the NINDS-SPSP international workshop. Neurology 1996; **47**:1–9.

24. Gilman S, Low PA, Quinn N et al. Consensus statement on the diagnosis of multiple system atrophy. J Auton Nerv Syst 1998;**74**:189–92.
25. Fujiwara T, Watanuki S, Yamamoto S et al. Performance evaluation of a large axial field-of-view PET scanner: SET-2400W. Ann Nucl Med 1997;**11**:307–13.
26. Kawamura K, Oda K, Ishiwata K. Age-related changes of the [11C]CFT binding to the striatal dopamine transporters in the Fischer 344 rats: a PET study. Ann Nucl Med 2003;**17**:249–53.
27. Hashimoto M, Kawasaki K, Suzuki M et al. Presynaptic and postsynaptic nigrostriatal dopaminergic functions in multiple system atrophy. Neuroreport 2008;**19**:145–50.
28. Ishibashi K, Ishii K, Oda K, Kawasaki K, Mizusawa H, Ishiwata K. Regional analysis of age-related decline in dopamine transporters and dopamine D(2)-like receptors in human striatum. Synapse 2008;**63**:282–90.
29. Staffen W, Mair A, Unterrainer J, Trinka E, Ladurner G. Measuring the progression of idiopathic Parkinson's disease with [123I] beta-CIT SPECT. J Neural Transm 2000; **107**:543–52.
30. Chouker M, Tatsch K, Linke R, Pogarell O, Hahn K, Schwarz J. Striatal dopamine transporter binding in early to moderately advanced Parkinson's disease: monitoring of disease progression over 2 years. Nucl Med Commun 2001;**22**:721–5.
31. Marek K, Innis R, van Dyck C et al. [123I]beta-CIT SPECT imaging assessment of the rate of Parkinson's disease progression. Neurology 2001;**57**:2089–94.
32. Lee CS, Samii A, Sossi V et al. In vivo positron emission tomographic evidence for compensatory changes in presynaptic dopaminergic nerve terminals in Parkinson's disease. Ann Neurol 2000;**47**:493–503.

Neuroradiologic Evidence of Pre-Synaptic and Post-Synaptic Nigrostriatal Dopaminergic Dysfunction in Idiopathic Basal Ganglia Calcification: A Case Report

Takahiro Saito, MD, Mitsuru Nakamura, MD, Teruhiko Shimizu, MD, Keiichi Oda, PhD, Kiichi Ishiwata, PhD, Kenji Ishii, MD, PhD, Kunihiro Isse, MD, PhD

From the Department of Psychiatry, Tokyo Metropolitan Toshima Hospital, Tokyo, Japan (TS, MN, TS, KI); and Tokyo Metropolitan Institute of Gerontology, Positron Medical Center, Tokyo, Japan (KO, KI, KI).

[Correction added after online publication 17-March-2010: Received date corrected.]

ABSTRACT

Idiopathic basal ganglia calcification (IBGC) is a neuropathological condition known to manifest as motor disturbance, cognitive impairment, and psychiatric symptoms. The pathophysiology of the psychiatric symptoms of IBGC, however, remains controversial. A previous biochemical study suggested that dopaminergic impairment is involved in IBGC. We thus hypothesized that dopaminergic dysfunction might be related with the psychiatric manifestations of IBGC. We used positron emission tomography to measure glucose metabolism and dopaminergic function in the basal ganglia of an IBGC patient with psychiatric symptoms. The results showed that widespread hypometabolism was evident in the frontal, temporal, and parietal cortices while the decline in dopaminergic function was severe in the bilateral striatum. The functional decline of the dopamine system in the calcified area of the bilateral striatum and the disruption of cortico-subcortical circuits may contribute to clinical manifestations of IBGC in our patient.

Keywords: Idiopathic basal ganglia calcification, catatonia, CFT, RAC, PET.

Acceptance: Received February 3, 2008, and in revised form July 29, 2008. Accepted for publication August 9, 2008.

Correspondence: Address correspondence to Takahiro Saito, Department of Psychiatry, Tokyo Metropolitan Toshima Hospital, Tokyo, Japan. E-mail: takahiro-s@toshima-hp.metro.tokyo.jp.

J Neuroimaging 2010;20:189-191.
DOI: 10.1111/j.1552-6569.2008.00314.x

Introduction

Idiopathic basal ganglia calcification (IBGC) is a neuropathological condition that sometimes manifests as a clinical syndrome characterized by motor disturbance, cognitive impairment, and psychiatric symptoms. The etiological relationship between IBGC and its psychiatric manifestations has been a topic of controversy.[1,2] Some authors have hypothesized that IBGC affects the integration of the cortical-subcortical circuits.[2-4] The psychiatric symptoms have been attributed to the disruption of the dopamine (DA) system. A biochemical study revealed an impaired nigrostriatal DA system.[5] A positron emission tomography (PET) study measuring [^{18}F]6-fluoro-L-dopa uptake revealed, however, an intact nigrostriatal pathway.[6] Thus, a direct association between IBGC and a dysfunction in the DA system has not been established yet.

In this study, we performed PET analysis to evaluate the glucose metabolism and the presynaptic and postsynaptic nigrostriatal DA function and their pathophysiological significance in an IBGC patient.

Case Report

A single 44-year-old woman was admitted after she attempted suicide. Over the past 2 decades, she had been hospitalized several times for a mood disorder with psychotic features. There was no family history of psychiatric or neurological disorders. On admission, the patient presented with agitation, suicidal ideation, disorganized thought, and echolalia. Her neurological examination revealed no abnormalities. Cranial radiography showed bilateral calcification of the striatum, and brain computed tomography revealed bilateral symmetrical calcification of the dentate nuclei of the cerebellum, caudate nuclei, putamen, globus pallidus, and the nuclei pulvinares thalami (Fig 1). Atrophy was not observed in the cerebral cortex. Laboratory findings, including serum and urine calcium and phosphate levels and serum parathyroid hormone levels, were normal. Her electroencephalogram was normal. Based on these findings, she was diagnosed with IBGC.

The patient received 4 mg/day of risperidone and 800 mg/day of lithium carbonate; her agitation and disorganized thinking were ameliorated within 2 weeks. However, she developed a drug-induced Parkinsonism that manifested as tremor, rigidity, shuffling gait, and dysphagia. Thus, the previous medication was tapered and switched to 50 mg/day of trazodone during a month period. Though the Parkinsonism described above temporarily improved, a catatonic syndrome such as stupor, echolalia, rigidity, and dysphagia ensued. A course of electro-convulsive therapy (ECT) was indicated for which informed consent was obtained from the patient's father. She was administered bitemporal ECT. After 8 sessions of ECT, she was completely relieved of catatonic symptoms.

PET scanning using [^{11}C]-labeled 2β-carbomethoxy-3β-(4-fluorophenyl)-tropane ([^{11}C]CFT), a ligand for the striatal pre-synaptic DA transporter, and [^{11}C]-labeled raclopride ([^{11}C]RAC), which binds DA D_2 receptors and reflects post-synaptic DA function, and [^{18}F]fluorodeoxyglucose ([^{18}F]FDG) was performed 1 month after the cessation of risperidone, when the patient exhibited a catatonic syndrome. Further, an [^{18}F]FDG-PET scan was obtained again one week after the last ECT session. The data acquisition methods have been described previously.[7,8] The study protocol was approved by the Ethics Committee of the Tokyo Metropolitan Institute of Gerontology, and informed consent was obtained from the patient's father.

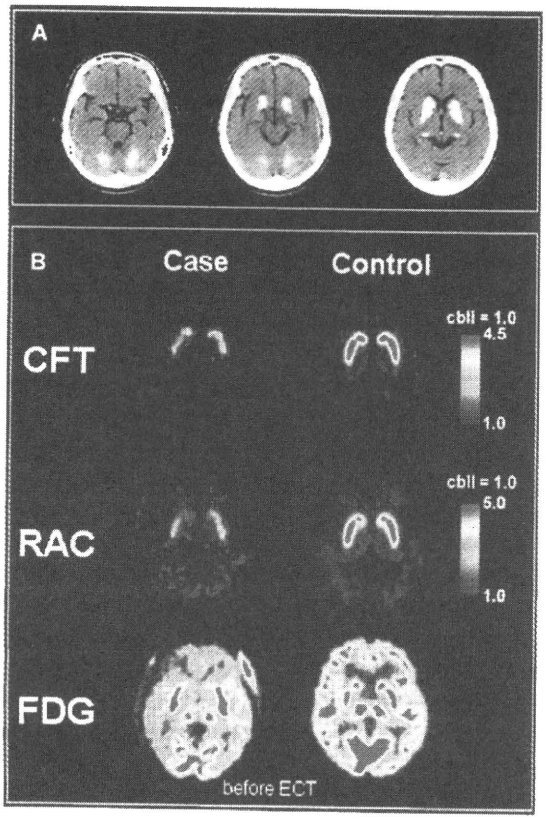

Fig 1. (A) Cranial CT images representing bilateral calcification of the striatum and the cerebellum. (B) PET images representing decreased uptake of [^{11}C]CFT, [^{11}C]RAC, and [^{18}F]FDG in the bilateral striatum. Images of [^{18}F]FDG-PET were based on the static distribution of [^{18}F]FDG activity.

The results showed significantly decreased accumulation of [^{11}C]CFT and [^{11}C]RAC in the bilateral striatum. The area demonstrating decreased uptake was consistent with the distribution of calcified region (Fig 1, Table 1). Widespread decreases in glucose uptake were observed in the bilateral cerebral cortices; prominent reduction was observed in the right prefrontal, temporal, and parietal cortices. After the final ECT session, improvement was observed in areas that had previously shown significant hypometabolism (Fig 2).

Discussion

An important limitation of this study is that the possible effect of antipsychotics on the DA D_2 receptors could not be eliminated. However, though the reported DA D_2 receptor occupancy of risperidone is about 79% at 24 hours after single oral administration of 3 mg,[9] we think that the interval after cessation of antipsychotics we took is appropriate for diminishing its effect on DA D_2 receptors. Furthermore, as trazodone at 2.5–20 mg/kg reportedly did not block DA D_2 receptors in rats,[10] it suggests that trazodone at 1mg/kg prescribed for this patient does not affect the result of [^{11}C]RAC-PET.

Previous imaging studies of IBGC with schizophrenia-like psychosis revealed abnormalities in the basal ganglia.[11,12] Casanova et al. suggested that abnormalities in iron metabolism may play a substantial role in the process of calcification and the dopaminergic dysfunction observed in IBGC patients with schizophrenia-like psychosis.[13] Thus, it is postulated that the process of mineralization precipitates neuronal degeneration, leading to the functional derangement of the basal ganglia in these patients. Our result indicated that the density of the DA transporter and DA D_2 receptor was decreased, resulting in a decline in pre- and post-synaptic DA functions in the bilateral striatum. Regarding the finding that the area which showed the functional derangement of DA system matched the distribution of calcification, DA dysfunction in our case might reflect the destruction of synaptic structure due to calcification.

A prominent feature in our case is the marked hypometabolism in the right frontal, temporal, and parietal cortices that improved after the ECT sessions along with a resolution of psychiatric symptoms. This finding is consistent with previous imaging studies that demonstrated the involvement of the orbitofrontal cortex and the right parietal cortex in catatonic patients.[14] Cortical alterations in our case may reflect a disruption of the cortico-subcortical circuits due to striatal dysfunction,

Table 1. Ratio Index for [^{11}C]CFT and [^{11}C]RAC, and Uptake Ratio of [^{18}F]FDG

Region of Interest (ROIs)	Ratio Index for [^{11}C]CFT		Ratio Index for [^{11}C]RAC		Uptake Ratio of [^{18}F]FDG			
	Case	Control (Mean ± SD)	Case	Control (Mean ± SD)			Case	Control (Mean ± SD)
Right caudate	2.26*	4.09 ± .77	1.95*	3.90 ± .58	Caudate	Before ECT	1.00*	1.39 ± .11
Left caudate	2.09*		2.05*			After ECT	1.08*	
Right anterior putamen	2.27*	4.24 ± .80	2.31*	4.53 ± .55	Anterior	Before ECT	1.21*	1.49 ± .11
Left anterior putamen	2.29*		2.28*		putamen	After ECT	1.14*	
Right posterior putamen	2.20*	3.99 ± .73	2.56*	4.45 ± .57	Posterior	Before ECT	1.55	1.51 ± .12
Left posterior putamen	2.19*		2.37*		putamen	After ECT	1.44	

For ratio index, the regions of interest (ROIs) were located in the caudate nucleus and the anterior and posterior part of the putamen on each side with reference to individual MR images. The ratio index of a target region was calculated by setting the cerebellum as the region of reference using simple ratio method. We then compared these values with those from age-matched control subjects (n = 14, ages 35-45). Uptake ratio of [^{18}F]FDG in the basal ganglia relative to the cerebellum was also calculated before and after ECT, then compared with the mean value in normal controls (the same cohort noted above). * 2 SD below the mean.

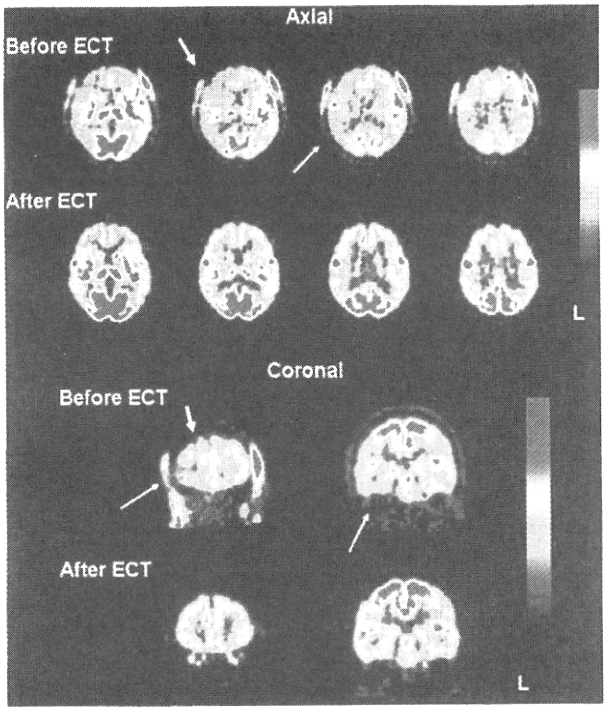

Fig 2. Axial and coronal images of [^{18}F]FDG PET before and after the ECT sessions indicating the improvement in regional hypometabolism in the right frontal, temporal, and parietal cortices after ECT (arrow).

in particular the lateral orbitofrontal loop that reciprocally connect the caudate nucleus with the lateral orbitofrontal cortex. Increased relative uptake of [^{18}F]FDG in the caudate nucleus after ECT further supports an involvement of the lateral orbitofrontal loop in the resolution of psychiatric symptoms.

Pre- and post-synaptic DA dysfunction in the putamen might affect the severity of motor symptoms such as rigidity and dysphagia of our case, for several neuroimaging studies had revealed loss of dopamine transporters in the putamen of patients with Parkinson's disease, progressive supranuclear palsy (PSP), and multiple system atrophy (MSA), as well as decreased DA D_2 receptors in patients with PSP and MSA.[15] In addition, decreased relative glucose uptake in posterior putamen after ECT observed in our case may reflect the clinical improvement of motor symptoms.

In conclusion, our results suggest that the functional decline in the DA system in the calcified area of the bilateral striatum contributed to clinical manifestations in our patient. However, further investigations with a larger sample size are warranted to elucidate the pathophysiology of IBGC.

References

1. Förstl H, Krumm B, Eden S, et al. What is the psychiatric significance of bilateral basal ganglia mineralization? *Biol Psychiatry* 1991;29:827-833.
2. López-Villegas D, Kulisevsky J, Deus J, et al. Neuropsychological alterations in patients with computed tomography-detected basal ganglia calcification. *Arch Neurol* 1996;53:251-256.
3. Cummings JL, Gosenfeld LF, Houlihan JP, et al. Neuropsychiatric disturbances associated with idiopathic calcification of the basal ganglia. *Biol Psychiatry* 1983;18:591-601.
4. Le Ber I, Marie RM, Chabot B, et al. Neuropsychological and ^{18}FDG-PET studies in a family with idiopathic basal ganglia calcification. *J Neurol Sci* 2007;258:115-122.
5. Savoldi F, Nappi G, Martignoni E, et al. Biochemical evidence of dopaminergic involvement in Fahr's syndrome. *Acta Neurol* 1980;2:231-239.
6. Manyam BV, Bhatt MH, Moore WD, et al. Bilateral striopallidodentate calcinosis: cerebrospinal fluid, imaging, and electrophysiological studies. *Ann Neurol* 1992;31:379-384.
7. Hashimoto M, Kawasaki K, Suzuki M, et al. Presynaptic and postsynaptic nigrostriatal dopaminergic functions in multiple system atrophy. *Neuroreport* 2008;19:145-150.
8. Suzuki Y, Mizoguchi M, Kiyosawa M, et al. Glucose hypermetabolism in the thalamus of patients with essential blepharospasm. *J Neurol* 2007;254:890-896.
9. Takano A, Suhara T, Ikoma Y, et al. Estimation of the time-course of dopamine D_2 receptor occupancy in living human brain from plasma pharmacokinetics of antipsychotics. *Int J Neuropsychopharmacol* 2004;7:19-26.
10. Balsara JJ, Jadhav SA, Gaonkar RK, et al. Effect of the antidepressant trazodone, a 5-HT 2A/2C receptor antagonist, on the dopamine-dependent behaviors in rats. *Psychopharmacology* 2005;179:597-605.
11. Hempel A, Henze M, Berghoff C, et al. PET findings and neuropsychological deficits in a case of Fahr's disease. *Psychiatry Res* 2001;108:133-140.
12. Shouyama M, Kitabata Y, Kaku T, et al. Evaluation of regional cerebral blood flow in Fahr disease with schizophrenia-like psychosis. *Am J Neuroradiol* 2005;26:2527-2529.
13. Casanova MF, Araque JM. Mineralization of the basal ganglia: implications for neuropsychiatry, pathology and neuroimaging. *Psychiatry Res* 2003;121:59-87.
14. Northoff G. Neuroimaging and neurophysiology. In: Caroff SN, Mann SC, Francis A, Fricchione GL, eds. *Catatonia. From Psychopathology to Neurobiology.* Arlington, VA: American Psychiatric Publishing, Inc., 2004: 77-91.
15. Shinotoh H. Neuroimaging of PD, PSP, CBD and MSA - PET and SPECT studies. *J Neurol* 2006;253:30-34.

Neurol Sci
DOI 10.1007/s10072-011-0479-6

CASE REPORT

Two cases of dementias with motor neuron disease evaluated by Pittsburgh compound B-positron emission tomography

Yoshihiro Yamakawa · Hiroyuki Shimada · Suzuka Ataka · Akiko Tamura · Hideki Masaki · Hiroshi Naka · Tsuyoshi Tsutada · Aki Nakanishi · Susumu Shiomi · Yasuyoshi Watanabe · Takami Miki

Received: 1 August 2010 / Accepted: 11 January 2011

Abstract We described the cases of two patients with dementia associated with motor neuron disease, the former with frontotemporal dementia (FTD) and the latter with Alzheimer's disease (AD), studied by the Pittsburgh compound B-positron emission tomography (PIB-PET). In the FTD patient, the PIB-PET revealed no amyloid accumulation in the cortex, whilst in the AD patient showed amyloid accumulation mainly in the frontal, parietal and lateral temporal lobes, besides the posterior cingulate gyrus and the precuneus. Thus, PIB-PET might facilitate the discrimination of different proteinopathies that cause neurodegenerative diseases, as dementia associated with ALS.

Keywords Pittsburgh compound B (PIB) · Amyotrophic lateral sclerosis · Alzheimer disease · Frontotemporal dementia · Motor neuron disease

Y. Yamakawa · H. Shimada (✉) · S. Ataka · A. Tamura · H. Naka · T. Tsutada · T. Miki
Department of Geriatric Medicine and Neurology, Osaka City University Graduate School of Medicine, 1-4-3 Asahi-machi, Abeno-ku, Osaka 545-8586, Japan
e-mail: h.shimada@med.osaka-cu.ac.jp

S. Shiomi
Department of Nuclear Medicine, Osaka City University Graduate School of Medicine, Osaka, Japan

H. Masaki · A. Nakanishi
Kosai-in Hospital, Osaka, Japan

Y. Watanabe
RIKEN Center for Molecular Imaging Science, Kobe, Japan

Y. Watanabe
Department of Physiology, Osaka City University Graduate School of Medicine, Osaka, Japan

Published online: 05 February 2011

Introduction

Some motor neuron diseases (MNDs) are accompanied by cognitive impairment and occasionally confused with Alzheimer's disease (AD). Frontotemporal dementia (FTD) can occur clinically in patients with MND in approximately 2% of sporadic amyotrophic lateral sclerosis (ALS) cases; this condition is called as FTD-MND [1]. On the other hand, some studies suggest that from one-third to half of the ALS patients have some types of cognitive impairments, including AD, throughout the clinical course, and many studies have indicated an overlap between ALS and cognitive impairment [2].

It has been reported that FDG-PET is useful for the differential diagnosis of several types of dementia, especially AD and FTD. Recently, Pittsburgh compound B-positron emission tomography (PIB-PET) has been used to evaluate the degree of amyloid accumulation in the brain. In general, AD is characterized by the accumulation of amyloid in the cortex of the frontal, parietal, and lateral temporal lobes, whereas this type of accumulation is not specific for FTD. Therefore, the evaluation of the cortex using PIB-PET could help us to understand the origin of the cognitive impairment.

We conducted PIB-PET study in two cases of dementia associated with MND to confirm the clinical significance of the PET study.

Case report

Case report 1

A 61-year-old man presented with cognitive impairment with muscle atrophy and muscle weakness of the first

dorsal interosseus; the condition had been progressive since October 2007. On admission to our hospital in 2008, the score for Hasegawa's Dementia Scale-Revised (HDS-R) was 11/30, and that for Mini-Mental State Examination (MMSE) was 15/30, in which recent memory, verbal recall, and orientation were mainly affected. Frontal signs such as forced laughter, personality disorder, and depressive mood were also observed. In addition, atrophy of the tongue, fasciculations in the thigh, and weaknesses of the distal muscles of the upper limbs, mainly in the first dorsal interosseus were observed. Jaw and knee reflexes were hyperactive, and both snout and tonic planter reflexes were present. However, sensory deficits were not detected. His medical history was unremarkable, and he had no family history of neurological diseases. He was diagnosed as the clinically probable ALS with the El-Escorial criteria [3] and refused the treatment with riluzole and had no treatment. Nerve conduction studies (NCS) were normal, while needle electromyography (EMG) studies showed both spontaneous activities and diffuse neurological changes in the extremities and trunk; these symptoms were compatible with MND. Magnetic resonance imaging (MRI) showed mild atrophy in both the frontal and parietal lobes and in the left hippocampus (Fig. 1). PIB-PET indicated no accumulation of amyloids in the cortex, while PET with 18F-fluorodeoxyglucose (FDG-PET) indicated depressed metabolism of glucose in the frontal and temporal lobes (Fig. 2); these signs were compatible with FTD. These findings suggested that the patient had FTD-MND.

Case report 2

A 79-year-old woman presented with cognitive impairment which had been progressive since September 2005. She developed bulbar palsy, including dysarthria and dysphagia, since December 2007 and March 2008, respectively. Initial evaluation in 2005 revealed that her HDS-R score was 25/30 and MMSE score was 25/30. The neurologic examination was normal. The diagnosis was mild cognitive impairment and, after 3 years, HDS-R was 21/30 and MMSE was 24/30, with disturbances in both recent memory and orientation. Atrophy and fasciculation of the tongue were observed, while mild muscle atrophy and weakness of the neck and both the upper limbs were observed. Deep tendon reflexes in both the upper limbs were hyperactive, and snout reflex was present. However, there were no sensory deficits. Her medical history was unremarkable, and she had no family history of neurological diseases. NCS were normal, whereas needle EMG studies revealed high amplitude, long duration, and polyphasic spontaneous activities in the upper extremities, although spontaneous activities were not found. These findings suggest that this patient was compatible to the clinically probable laboratory- supported ALS with the El-Escorial criteria [3] with the one lesion showed the upper and lower motor signs. Brain MRI showed mild atrophy in both the left and right hippocampus and diffuse atrophy in the cerebral cortex consistent with her age (Fig. 3). PIB-PET indicated accumulation of amyloids mainly in the frontal lobe, anterior

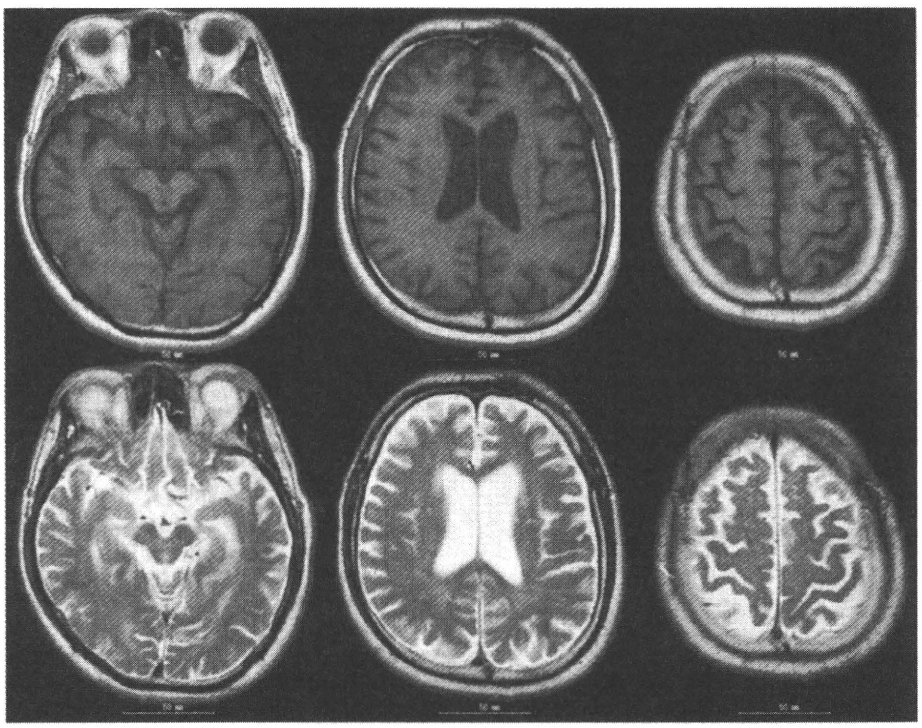

Fig. 1 Mild atrophy of both the frontal and parietal lobes and the left medial temporal area